

PROCEEDINGS OF THE XX ALL-RUSSIA CONFERENCE
ON PHYSICS OF FERROELECTRICS (VKS-XX)
(Krasnoyarsk, Russia, August 18–22, 2014)

Influence of the Electrical Conductivity on Dielectric Characteristics of a Triglycine Sulfate Crystal over a Wide Frequency Range

G. I. Ovchinnikova^a, I. Yu. Polyakova^a, E. S. Ivanova^{b,*}, R. V. Gainutdinov^b,
N. V. Belugina^b, A. L. Tolstikhina^b, and V. V. Grebenev^b

^a *Moscow State University, Moscow, 119991 Russia*

^b *Shubnikov Institute of Crystallography, Russian Academy of Sciences, Leninskii pr. 59, Moscow, 119333 Russia*

* *e-mail: ivanova.el.ser@gmail.com*

Abstract—The dielectric spectra of ferroelectric triglycine sulfate crystals were measured in the frequency range from 10 to 10¹¹ Hz and analyzed based on the concept of a significant contribution of the conductive component to the dielectric response of ferroelectrics. Images of lenticular ferroelectric domains in sulfate triglycine crystals were obtained using scanning spreading resistance atomic force microscopy, and background currents (10⁻¹⁴ A) and currents at domain walls (10⁻¹² A) were measured. It was shown that the inclusion of the contribution from the electrical conductivity to the dielectric spectra is in good agreement with the experimental data and provides additional information on the temperature dynamics of the domain structure.

DOI: 10.1134/S1063783415030191

1. INTRODUCTION

In recent years, an increasing interest has been expressed in the study of the role of electrical conductivity in pretransition regions of ferroelectric phase transitions [1, 2]. The first indications of electrical conduction in the vicinity of ferroelectric phase transitions were revealed in dielectric spectra of some ferroelectrics measured in the microwave range [3, 4]. It was found that, in temperature dependences of dielectric permittivity ϵ in the immediate vicinity of the phase transition (beginning with the frequency of 10⁹ Hz), there is a dip in the values of ϵ down to values below the level of the high-frequency contribution of ϵ_∞ and even to negative values. The question about the nature of this phenomenon has remained open until now. It is believed that, near the phase transition, there is a “slowdown” of the relaxation time. This phenomenon is determined by the Debye model, which is most adequately describes dielectric spectra of ferroelectrics over the entire range of the relaxation response. However, the mechanism of the observed “slowdown” is not fully understood. In this approach, deviations from the Debye model are explained by different distributions of the relaxation times and described by different empirical formulas [5]. Previously, attempts to describe specific features of the microwave dielectric response in terms of the conductive component could be justified by only indirect evidence. Currently, there is a real opportunity to solve this problem using atomic force microscopy (AFM). The AFM method makes it possible not only to reveal electrical conduction but also, in some modes, to identify regions where electrical conduction occurs [1].

In this study, an attempt has been made to analyze the role of electrical conductivity in the ferroelectric phase transition for a ferroelectric triglycine sulfate (TGS) crystal used as an example by measuring the dielectric spectra over a wide frequency range with invoking the electrical conductivity data obtained from special AFM investigations of the dynamics of the domain structure.

2. EXPERIMENTAL SETUPS AND MEASUREMENT TECHNIQUES

Dielectric spectra, i.e., temperature–frequency dependences of the real and imaginary parts of the dielectric permittivity, were measured in the frequency range from 10 to 10¹¹ Hz at temperatures in the range from room temperature to the phase transition point. We used three experimental setups for measurements in different frequency ranges. At low frequencies (to 10⁶ Hz), the measurements were carried out using impedance spectroscopy on a Novoterm-1200 with an Alpha-AN impedance analyzer. The complex permittivity of single-crystal TGS samples was measured during stepwise heating under temperature stabilization conditions in the range of 293–330 K. The samples were cut in the form of 1-mm-thick plane-parallel plates (5 × 5 mm in size) with large faces oriented perpendicular to the *Y* axis. Silver paste was used as electrodes. In the microwave range, different measurement techniques were used depending on the frequency range under investigation. At frequencies in the range from 10 to 50 GHz, the permittivity was measured by the short-circuited waveguide method.

In this case, a 4-mm-thick crystal was cut in accordance with the size of the waveguide with the corresponding cross section and placed at the short-circuited end of the waveguide, followed by measuring changes in the distribution of the field in the waveguide with the crystal as compared to the unloaded waveguide [4]. In the frequency range from 90 to 150 GHz, the permittivity was measured on a submillimeter spectrometer based on a backward-wave tube [6]. The frequency-tunable monochromatic radiation in the form of a 40-mm-diameter beam formed by dielectric lenses was propagated in free space and normally incident on a 5.22-mm-thick sample plate with a cross section of 10.70×12.43 mm. The radiation transmitted through the sample was recorded on a photoacoustic detector. The spectra $\varepsilon'_m(\omega)$ and $\varepsilon''_m(\omega)$ were calculated with the "Epsilon 2001" software. The AFM measurements were performed using the methods described in [2].

All the experiments were performed on TGS crystals grown at the Shubnikov Institute of Crystallography of the Russian Academy of Sciences (Moscow, Russia) by means of isothermal evaporation at a temperature below the phase transition temperature T_c ($T < T_c$). The TGS crystal is a uniaxial ferroelectric with a second-order ferroelectric phase transition at a temperature of 49°C and belongs to ferroelectrics with hydrogen bonds, in which the proton subsystem has a significant influence on the phase transition. In all the experimental techniques, before performing measurements the crystals were annealed at a temperature of 110°C for 2 h, and the measurements were carried out with a stepwise increase in the temperature.

3. RESULTS AND DISCUSSION

The dielectric spectra of the TGS crystal measured in the low-frequency range from 10 to 10^6 Hz at temperatures from room temperature to the phase transition point are shown in Fig. 1. These spectra have the following characteristic features: (1) the low-frequency dielectric relaxation dispersion is observed at frequencies up to 10^5 Hz and at temperatures from room temperature to 36°C and is absent at higher temperatures, including the phase transition temperature; and (2) the dielectric response at frequencies of 10^6 Hz has the vibrational component with a clear increase in the amplitude of the response when approaching the phase transition temperature (above T_c , the vibrational component disappears).

Figure 2 shows the dielectric spectra measured in the microwave range for two characteristic temperatures (24 and 46°C) at which the low-frequency dielectric spectra have a different behavior. It should be noted that there is a good quantitative agreement between the values of ε' at the high-frequency boundary of the low-frequency dielectric spectra and the values at the low-frequency boundary of the microwave

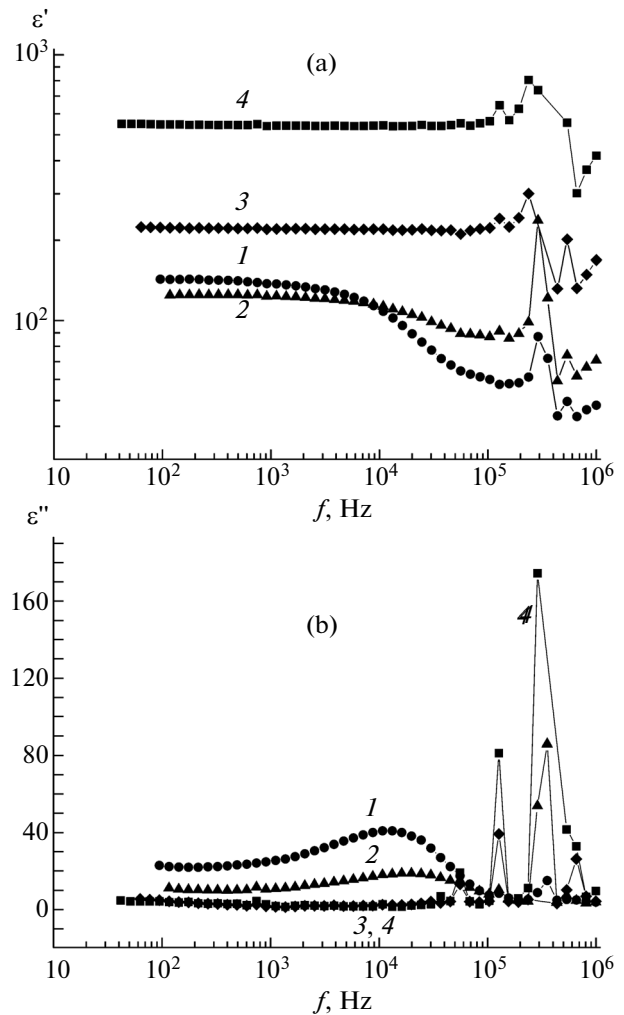


Fig. 1. Experimental frequency dependences of the (a) real part ε' and (b) imaginary part ε'' of the permittivity at different temperatures $T = (1)$ 24, (2) 35.8, (3) 46, and (4) 49.1°C.

dielectric spectra, which indicates the absence of a significant dispersion in the frequency range not studied in our work. In the microwave range, the dielectric relaxation dispersion also occurs, but its temperature dynamics differs from the low-frequency dynamics. First of all, in this frequency range, the dispersion takes place for all the studied temperatures up to the phase transition temperature. At room temperature, the microwave dielectric spectra are similar to the low-frequency dielectric spectra measured at a temperature of 24°C, whereas the dielectric spectra obtained at a temperature of 46°C exhibit specific features that are not typical both for low-frequency dielectric spectra and for the relaxation dielectric response. Starting with the frequency of 10 GHz, the permittivity ε' decreases sharply and, at a frequency of 40 GHz, becomes below the level of ε_∞ . For some crystals, the permittivity ε' has negative values.

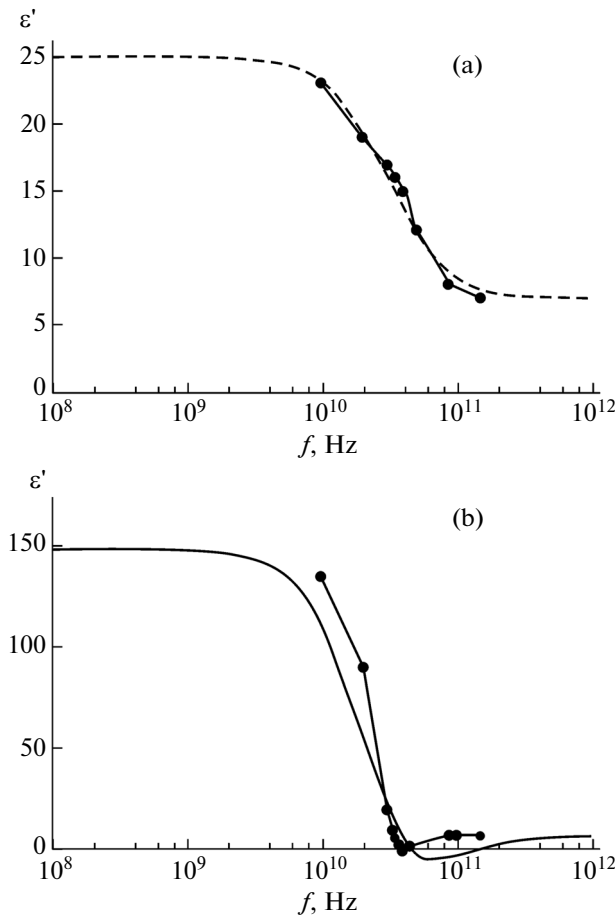


Fig. 2. Frequency dependences of the real part of the permittivity ϵ' in the microwave range at temperatures $T =$ (a) 24 and (b) 46°C. Points are the experimental data. The dashed line shows the results of the calculation within the Debye model (the first term in formula (4)) with the parameters $\epsilon(0) = 25$, $\epsilon_\infty = 7$, and $\tau_1 = 5 \times 10^{-12}$ s. The solid line shows the results of the calculation using formula (4) with the parameters $\epsilon(0) = 200$, $\epsilon_\infty = 7$, $\tau_1 = 8 \times 10^{-12}$ s, $\sigma_0 = 3.4 \times 10^{-3}$ ($\Omega \text{ m}$) $^{-1}$, and $\tau_2 = 2 \times 10^{-12}$ s.

A new information about domain walls was provided by scanning resistive probe microscopy scanning. The sample was placed on a substrate with a contact in the form of a conductive adhesive tape used as the first electrode, to which the bias voltage (10 V) was applied. A conductive probe serving as the second electrode was used to measure the resulting current flowing through the sample. For the first time, we obtained a spreading resistance AFM image of a lenticular ferroelectric domain (Fig. 3) in the TGS crystal [2]. Contrast at domain walls was caused by an increased intensity of the current in the domain wall region (the background current was 10^{-14} A, and the current at domain walls was 10^{-12} A). Previously, in the literature, assumptions were made about the existence of charged domain walls [7]. Based on the AFM data, it can be concluded that domain walls possess

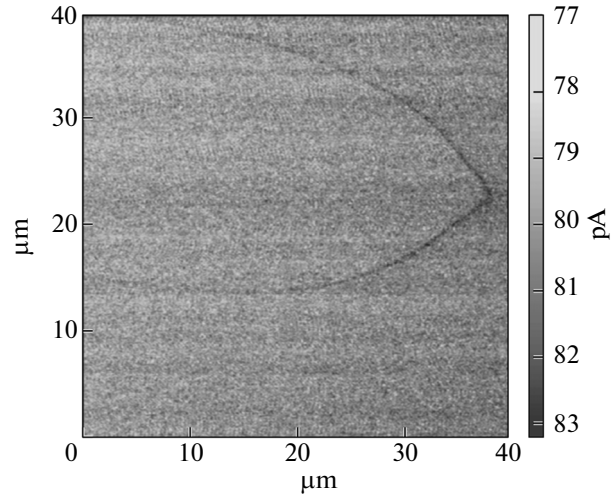


Fig. 3. Spreading resistance AFM image of a lenticular domain in the TGS crystal.

increased conductivity. As compared with the electrical conductivity of the crystal, the conductivity of domain walls proved to be higher. This opens up possibilities for controlling the local conductivity of domain walls and constructing the corresponding surface current distributions.

Let us discuss the experimental dielectric spectra of the ferroelectric TGS crystal within the concept that, in the dielectric response, there are simultaneously two dispersion mechanisms, namely, the relaxation orientation mechanism, which is characteristic of dielectrics, and the mechanism associated with electrical conduction. The dielectric response of the orientation component will be described by the Debye model of rotation of dipoles in a viscous medium, in which the dependence of the permittivity ϵ^* on the frequency ω has the form

$$\epsilon^* = \epsilon_\infty + \frac{\epsilon'(0) - \epsilon_\infty}{1 + i\omega\tau_1}, \tag{1}$$

and the dielectric response of the conductive component σ^* will be described by the Drude model of motion of charge carriers in a viscous medium:

$$\sigma^* = \frac{\sigma_0}{1 - i\omega\tau_2}. \tag{2}$$

Here, $\epsilon'(0)$ and ϵ_∞ are the static and high-frequency components of the permittivity, respectively; σ_0 is the frequency-independent conductivity; and τ_1 and τ_2 are the relaxation times in the Debye model and the Drude model, respectively. The relationship between ϵ^* and σ^* can be represented by the classical expression

$$\epsilon^* = \frac{-i\sigma^*}{\epsilon_0\omega}. \tag{3}$$

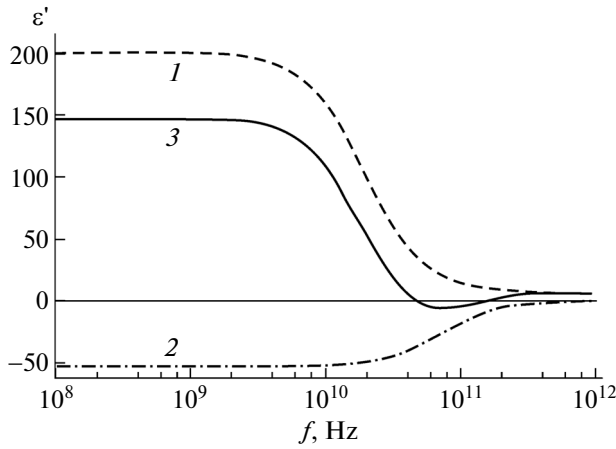


Fig. 4. Frequency dependences of the real part of the permittivity ε' calculated according to (1) Debye model (the first term in formula (4)) with the parameters $\varepsilon(0) = 200$, $\varepsilon_\infty = 7$, and $\tau_1 = 8 \times 10^{-12}$ s; (2) Drude model with the parameters $\sigma_0 = 3.3 \times 10^{-3}$ ($\Omega \text{ m}$) $^{-1}$ and $\tau_2 = 2 \times 10^{-12}$ s; and (3) formula (4) with the same parameters.

After the separation of the real and imaginary parts of the equations, we obtain the frequency dependences of the permittivities ε' and ε'' in the following form:

$$\varepsilon'(\omega) = \varepsilon_\infty + \frac{\varepsilon'(0) - \varepsilon_\infty}{1 + \omega^2 \tau_1^2} - \frac{\sigma_0 \tau_2}{\varepsilon_0 (1 + \omega^2 \tau_2^2)}, \quad (4)$$

$$\varepsilon''(\omega) = \frac{(\varepsilon'(0) - \varepsilon_\infty) \omega \tau_1}{1 + \omega^2 \tau_1^2} + \frac{\sigma_0}{\varepsilon_0 \omega (1 + \omega^2 \tau_2^2)}. \quad (5)$$

From expressions (4) and (5), it can be seen that the contribution from each of the mechanisms to the dielectric response of the real and imaginary parts of the permittivity is different: the contributions from both mechanisms to the imaginary part of the permittivity ε'' are always positive, while the contributions to the real part of the permittivity ε' have opposite signs, so that the permittivity ε' can be either negative or positive. Far from the dispersion regions ($\omega\tau < 1$), where the permittivity does not depend on the frequency, the signs of $\varepsilon'(\omega)$ will always be determined by the dominant contribution to the major mechanism of the dielectric response, and the observation of the small contribution from the minor mechanism, even with the opposite sign, can be a difficult task, if there is no other evidence for its presence in the spectrum. In the regions of strong dispersion ($\omega\tau \sim 1$), where the contribution from the major mechanism decreases with an increase in the frequency, the minor mechanism with specific parameters for both dispersion mechanisms can manifest itself as a maximum or a minimum on the background of the decreasing contribution from the major mechanism of the dispersion. As an example, Fig. 4 shows the frequency dependences of the real part of the permittivity ε' , which were calculated sepa-

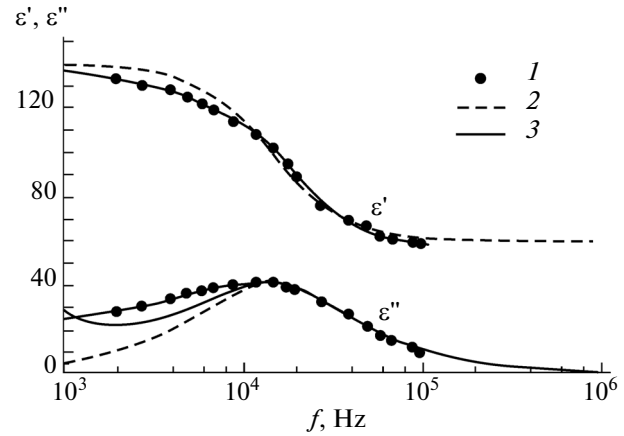


Fig. 5. Frequency dependences of the real part ε' and imaginary part ε'' of the permittivity at a temperature of 24°C: (1) experiment; (2) calculation in the Debye model with the parameters $\varepsilon(0) = 140$, $\varepsilon_\infty = 60$, and $\tau_1 = 1 \times 10^{-5}$ s; and (3) calculation using formulas (4) and (5) with the parameters $\varepsilon(0) = 140$, $\varepsilon_\infty = 60$, $\tau_1 = 1 \times 10^{-5}$ s, $\sigma_0 = 3.3 \times 10^{-3}$ ($\Omega \text{ m}$) $^{-1}$, and $\tau_2 = 2 \times 10^{-12}$ s.

rately for the contribution from the Debye component, the conductive component, and the total spectrum in the microwave range. The calculation was performed for the case where the Debye mechanism is dominant, and the relaxation time in this model is taken to be longer than the relaxation time in the Drude model. It can be seen from Fig. 4 that, at the high-frequency of the total spectrum, there is a minimum that visualizes the response of the conductive components against the background of the more rapidly decreasing orientation response.

Now, we apply this approach to the calculation of the experimental low-frequency dielectric spectra. Figure 5 shows the experimental and calculated frequency dependences $\varepsilon'(\omega)$ and $\varepsilon''(\omega)$ at a temperature of 24°C. It can be seen that the frequency dependence $\varepsilon'(\omega)$ is well approximated by the Debye model with a single relaxation time, while the frequency dependence $\varepsilon''(\omega)$ exhibits large deviations from this model at the low-frequency boundary. Therefore, the dependence $\varepsilon''(\omega)$ was calculated taking into account the contribution from the conductive components according to formula (5). The value of σ_0 was taken from our previous work [8], where we measured the static (or, in the terminology used in [9], through) conductivity of the TGS crystals. Taking into account the AFM data, according to which the current at domain walls is two orders of magnitude higher than the background current, we recalculated the through conductivity, which in the calculations was 10^{-10} ($\Omega \text{ m}$) $^{-1}$.

Next, we turn to the calculation of the microwave dielectric spectra. The Debye model with a single relaxation time serves as a good approximation for both the dependence $\varepsilon'(\omega)$ (Fig. 2) and the dependence

$\varepsilon''(\omega)$ at a temperature of 24°C. The dielectric spectrum at a temperature of 46°C could be described by using only the conductive component. In this case, the value of σ_0 , which was used in the approximation of the spectrum $\varepsilon'(\omega)$, is several orders of magnitude greater than the values of the static conductivity. Furthermore, the approximation of the frequency dependence $\varepsilon''(\omega)$ at this temperature also requires a different (two orders of magnitude smaller) value of σ_0 . Thus, the experiment and its interpretation using the electrical conductivity indicate that, in the ferroelectric TGS crystal, there are two types of conductivity: the time-independent static or through conductivity and the time-dependent dynamic conductivity. Note also that the frequency (time) contributions from the dynamic conductivity to $\varepsilon'(\omega)$ and $\varepsilon''(\omega)$ have a different character. These processes are considered as “transit effects,” the character of the frequency dependences of which is determined by the relationship of the residence time of charge carriers in the quasi-free state (time of flight) with the period of the external field [10].

Although there is an apparent (at first glance) inconsistency between the dielectric dispersion of the low-frequency spectra and the dielectric dispersion of the microwave spectra, they do provide additional information for the understanding of the temperature dynamics of the processes of ordering and disordering of the structure in the TGS crystals. At a low temperature and a small diffusion, there are both the low-frequency and high-frequency dispersions, which reflect the processes of ordering of structural units along the external field. At the same time, even a very low through conductivity, if it exists, manifests itself in the low-frequency spectra in the form of additional losses at the low-frequency boundary of these spectra and in the absence of these losses in the microwave spectra due to the inverse dependence on the frequency. An increase in the temperature leads to an increase in the diffusion and the number of dipoles able to be aligned with the field; i.e., the frequency-independent dielectric response of the system increases, whereas the dispersion decreases and disappears at higher temperatures, which can be seen from the curve at ~36°C (Fig. 1). Thus, at high temperatures, the number of dipoles aligned with the field is large enough and the low-frequency dispersion is absent. In this case, the microwave spectra exhibit dynamic conductivity (the permittivity ε' is negative). Possibly, this situation is associated with the fact that, as the temperature increases above 35°C, the domain structure undergoes a refinement: the number of domains and the density of domain walls increase. This can be responsible for the increase in both the through and, especially, dynamic conductivities. With a further increase in the temperature, the number of domains and the density of domain walls can reach the limiting values, when the crystal will begin to get rid of excess “defects,” passing into a more equilibrium state. This process manifests itself in the form of increasing resonant

vibrations at the high-frequency boundary of the low-frequency dielectric spectra as well as in the form of a minimum in the temperature–frequency dependence of ε' in the microwave dielectric spectrum. This minimum is observed at a temperature below the phase transition point, which can be considered as an indirect indication of the transition of the crystal into the quasi-equilibrium state. Of course, the presented picture of the dynamics of the structure requires further investigation and confirmation by performing both the AFM study of the temperature dynamics of the domain structure and the analysis of the dielectric spectra with an increase in the range toward lower and higher frequencies. Additional information can be obtained by comparing the spectra of undoped and doped crystals. And this is the aim of further research.

4. CONCLUSIONS

The performed analysis of the dielectric spectra of TGS crystals measured over wide ranges of frequencies and temperatures provides a better understanding of the dynamics of the domain structure. The investigations have demonstrated the importance of performing the simultaneous analysis and comparison of the low-frequency and ultra-high-frequency (microwave) dielectric spectra. An important role in confirming the validity of the proposed approach belongs to the results of AFM investigations of the electrical conductivity, which were used in calculating the dielectric spectra.

REFERENCES

1. G. I. Ovchinnikova, Yu. F. Korosteleva, and A. N. Sandalov, *Phys. Solid State* **35** (9), 1259 (1993).
2. A. L. Tolstikhina, Extended Abstract of the Doctoral Dissertation (Institute of Crystallography, Russian Academy of Sciences, Moscow, 2013).
3. L. P. Pereverzeva and Yu. M. Poplavko, *Sov. Phys. Crystallogr.* **18** (4), 492 (1978).
4. G. I. D'yakov, Extended Abstract of the Candidate's Dissertation (Moscow State University, Moscow, 1985).
5. Yu. M. Poplavko, L. P. Pereverzeva, and I. P. Raevskii, *Physics of Active Dielectrics* (Southern Federal University, Rostov-on-Don, 2009) [in Russian].
6. S. V. Danilova, E. S. Ivanova, A. K. Malyshev, G. I. Ovchinnikova, and Yu. A. Pirogov, *Phys. Wave Phenom.* **21**, 231 (2013).
7. A. K. Tagantsev, L. E. Cross, and J. Fousek, *Domains in Ferroic Crystals and Thin Films* (Springer-Verlag, New York, 2010).
8. G. I. Ovchinnikova and N. D. Gavrilova, *Ferroelectrics* **167**, 129 (1995).
9. A. S. Bogatin, I. V. Lisitsa, and S. A. Bogatina, *Tech. Phys. Lett.* **28** (9), 779 (2002).
10. S. D. Gvozdover, *The Theory of Microwave Frequency Electronic Devices* (GITTL, Moscow, 1956), p. 154 [in Russian].

Translated by O. Borovik-Romanova